Mars Background Noise Temperatures Received by Spacecraft Antennas

C. Ho,[1] S. Slobin,[1] M. Sue,[1] and E. Njoku[2]

Radio noise emissions seen by a spacecraft orbiting Mars or a lander located on the Martian surface are expected to be from Mars' atmospheric emission, surface noise, and extra-Martian sources. Compared with Earth, Mars has lower surface temperatures and much lower atmospheric absorption and radiation. However, Mars has higher surface emissivity due to the roughness of soil and rocks. Because of very low atmospheric density and optical depth, Mars' atmospheric emission from oxygen and water vapor is almost negligible. The upwelling brightness temperature at Mars is caused mainly by its surface temperature, with strong local time and latitudinal dependence. Downwelling brightness temperature is dominated by sky temperature. The actual radio noise contributing to the antenna temperature is also a function of antenna orientation, elevation angle, and gain pattern. Assuming a dish antenna with 1-m diameter, for a downward-looking antenna the total noise temperature is about the same as the Earth's for all frequency bands of interest, with ±15 percent deviations. For an upward-looking antenna, the noise temperature is less than half that of Earth.

I. Introduction

Recently, NASA decided to accelerate its pace of Mars exploration, and current plans are to send spacecraft to Mars every 1 or 2 years and ultimately to land humans on Mars around the year 2020. To carry out each mission successfully, telecommunication with the spacecraft is crucial. For this purpose, JPL is conducting studies to enhance communications [1] and navigation capabilities on or around Mars for future Mars missions and is investing in hardware development for use by those missions. In order to accomplish this task, it is necessary to fully understand the Martian environment (such as Martian surface and atmospheric radiation) and its effects on communication systems and subsystems on the spacecraft. This is also important in planning future Mars remote-sensing missions [2].

As the technology is continuously improved, space-qualified receiver noise temperature can be reduced to as low as 100 K [3]. Thus, actual receiver antenna temperature due to outside radio emission becomes more important. It is necessary to find out what the radio noise-temperature range is on Mars and how

[1] Communications Systems and Research Section.

[2] Earth Sciences Section.

The research described in this publication was carried out by the Jet Propulsion Laboratory, California Institute of Technology, under a contract with the National Aeronautics and Space Administration.

strong these emissions are in comparison with Earth's. In order to design highly qualified receivers for future Mars missions, it is also necessary to accurately determine the antenna temperature on the Martian surface and in Mars orbit.

The physical environment of Mars is significantly different from that of Earth in its surface features and atmosphere. Electromagnetic radiation on Mars is also different from that on Earth. Radio noise emissions at Mars basically include three types of sources [4]: Martian atmospheric emission, noise from the Martian surface, and extra-Martian sources. The Martian atmosphere has a gaseous attenuation due to the absorption by oxygen and water vapor, hydrometeors, and aerosols. These components also radiate noise at the same frequencies. Martian surface emissivity is closely related to its surface physical temperature and materials. Below a frequency of 1 GHz, the noise is mainly dominated by galactic radio sources. Actual radio noise temperature received by an antenna on a Mars orbiter or on the Martian surface is strongly dependent on antenna pointing, size, elevation angle, gain pattern, and radio frequency. Assuming a receiving dish antenna with a fixed 1-m diameter, using newly developed Martian atmospheric gaseous attenuation models, we can calculate the background noise temperatures seen by upward- and downward-looking antennas, as described below.

II. Antenna Temperature and Brightness Temperatures

A. Antenna Temperature [2,3]

The Martian background noise temperature seen by the receiving antenna (or antenna temperature) is defined as (see Fig. 1):

$$T_r = \frac{\int_\Omega G_r(\theta) T_B(\theta) d\Omega}{\int_\Omega G_r(\theta) d\Omega} \tag{1}$$

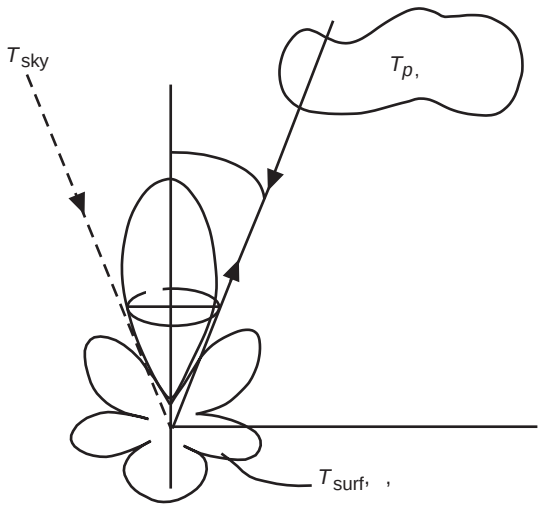

Fig. 1. Radio emission seen by an upward-looking beam antenna. Antenna temperature is the convolution of background brightness temperature and antenna gain in all directions.

where

$T_r =$ received noise temperature, K

$G_r =$ receiver antenna gain pattern, dimensionless

$T_B =$ brightness temperature, K

$d\Omega =$ solid angle, $\int_\Omega d\Omega = \int_0^\pi \int_0^{2\pi} \sin\theta d\theta d\phi = 4\pi$

$\theta =$ polar angle, 0 deg to 180 deg

$\phi =$ azimuth angle, 0 deg to 360 deg

The integration is over the entire sphere and includes the antenna's main beam and side lobes.

B. Upwelling and Downwelling Brightness Temperatures [4]

For an upward-looking antenna, the downwelling brightness temperature is

$$T_{B_d} = T_{\text{sky}} e^{-\tau} + T_a\left(1 - e^{-\tau}\right) \tag{2}$$

For a downward-looking antenna, the upwelling brightness temperature, including reflection from the surface, is

$$T_{B_u} = \varepsilon T_s e^{-\tau} + T_a\left(1 - e^{-\tau}\right) + T_{B_d}(1-\varepsilon)e^{-\tau} \tag{3}$$

where

$\varepsilon =$ surface emissivity, a function of frequency also depending on surface soil type, roughness, dielectric constant, moisture, etc., $0 \le \varepsilon \le 1$

$T_s =$ surface physical temperature (the average is 215 K on Mars and 300 K on Earth)

$\tau =$ atmosphere optical depth, a function of frequency and elevation angle, depending on cloud amount, gaseous absorption, etc. A nearly transparent object has a very small τ.

$T_a =$ mean physical temperature of the atmosphere (the average is 200 K on Mars and 230 K on Earth)

$T_{\text{sky}} =$ sky temperature as a function of frequency

Three types of temperature contribution to the brightness temperature received by an upward-looking antenna are shown in Fig. 1.

C. Receiving Antenna Model

We have used the antenna gain (G_t dBi) model recommended in ITU-R F.1245 [5] in this article, for which a 1-m-diameter dish antenna has been assumed. Expressing the gain as a function of polar angle, θ,

$$
\left.
\begin{aligned}
G_t(\theta) &= G_{\max} - 2.5 \times 10^{-3} \left(\frac{D}{\lambda}\theta\right)^2, \quad \text{for } 0 \text{ deg } \le \theta < \theta_m \\
G_t(\theta) &= 39 - 5\log\left(\frac{D}{\lambda}\right) - 25\log\theta, \quad \text{for } \theta_m \le \theta < 48 \text{ deg} \\
G_t(\theta) &= -3 - 5\log\left(\frac{D}{\lambda}\right) = G_{\min}, \quad \text{for } 48 \text{ deg } \le \theta \le 180 \text{ deg}
\end{aligned}
\right\} \tag{4}
$$

where the main-lobe gain is $G_{\max} \approx 20\log(D/\lambda)+7.7$ dBi; D is the antenna diameter; λ is the wavelength; the first side-lobe angle is $\theta_m = (20\lambda/D)\sqrt{G_{\max} - 2 - 15\log(D/\lambda)}$, which defines the main beam; and the half-power beamwidth is $69.3\lambda/D$ deg. An omni-directional antenna is assumed only for 400 MHz (UHF-band). All antenna parameters are listed in Table 1.

Table 1. Antenna gains for various frequency bands (D = 1.0 m).

Parameter	UHF-band	S-band	X-band	Ka-band	Omni-directional (UHF)
f, GHz	0.4	2.3	8.4	32	0.4
λ, cm	75	13	3.6	0.94	75
D/λ	1.33	7.7	27.7	106	—
$G_{\max}$, dBi	10.2	25.4	36.5	48.2	3
$G_{\min}$, dBi	−3.6	−7.4	−10.2	−13	−1
θ_m, deg	38	8.3	2.6	0.75	—
Half-power beamwidth, deg	52	9	2.5	0.65	∼60–90

D. Integration Areas

It is assumed that the satellite's orbit height around Mars is 890 km. When its antenna points downward, the main beam, which is defined by the first null, will illuminate a circular area with a radius of 10.1 km for 32 GHz (Ka-band) and 141 km for 2.3 GHz (S-band). Emissions from this area will have a dominant contribution to the integration of Eq. (1).

III. Mars Emissions

A. Mars Atmospheric Emission

The essential work of this study is to estimate the radio noise temperature radiated from the Martian atmosphere. At first the Martian atmospheric gaseous absorption coefficient (or specific attenuation) is calculated through a comparison with Earth's atmosphere. Then the atmospheric opacity $\tau(f)$ (or optical depth) at zenith is determined. Using these parameters, brightness temperatures can be obtained, representing the upwelling and downwelling atmospheric radiation.

1. Mars Atmospheric Gaseous Absorption Coefficient (Or Specific Attenuation). Attenuation and radiation from atmospheric molecules are heavily dependent on atmospheric structure [6], including atmospheric temperature, pressure, composition, abundance, etc. The atmosphere of Mars is

quite different from that of Earth in composition, abundance, and altitude profiles [7–9]. It is composed primarily of carbon dioxide, with small amounts of other gases. Because the Martian troposphere consists of almost entirely dry "air" and the surface atmospheric water content is 3000 times lower than at Earth [10], the absorption and radiation by hydrometeors are very low. Thus, the windows on Earth that are bounded by water lines become much wider on Mars. From 60 GHz to 180 GHz, there is almost no attenuation. This feature is obviously in contrast to the Earth's situation, in which clouds and water vapor dominate the attenuation. At Mars no rain observation has been reported yet. Even though it is possible to have rain, the rain would be so light that it would not cause any significant attenuation to radio waves. The Martian atmosphere is dominated by CO_2 and N_2 gases [11,12], which normally do not have electric or magnetic dipoles and so do not absorb electromagnetic energy. In this calculation, we have used an average surface value (300 ppm) for Martian water vapor instead of a maximum value (400 ppm), which corresponds to the worst case [13]. The ratio of total zenith absorption in the Earth atmosphere relative to Mars should be equal to the ratio of column number densities of H_2O and O_2 of Earth relative to Mars.

The first five major constituents in the Martian atmosphere are carbon dioxide (CO_2), 95.32 percent; nitrogen (N_2), 2.7 percent; argon (Ar), 1.6 percent; oxygen (O_2), 0.13 percent; and carbon monoxide (CO), 0.08 percent. Mars' surface pressure is ∼6.1 mb (variable); its surface atmospheric density is ∼0.020 kg/m^3; and its scale height is ∼11.1 km. The surface temperatures range from 184 K to 242 K with an average temperature of ∼215 K at low latitudes. The mean atmospheric physical temperature at one scale height is about 200 K.

From Table 2, it is seen that the Martian surface atmospheric pressure is only about 6/1000 of Earth's. Mars' average atmospheric molar weight (gram/mole) is larger than on Earth because the dominant gas, CO_2, has a larger molecular weight than does N_2 on Earth. However, its mole volume is much larger (by three orders of magnitude) than on Earth. Because of low pressure at Mars, the mass density of the Martian atmosphere is 61 times less than that of Earth. Thus, the average particle density is also smaller by about two orders of magnitude. Scale heights of both planetary atmospheres are only slightly different.

Table 3 lists various ratios of atmospheric compositions of Earth and Mars. These ratios are important factors related to atmospheric attenuation at both planets. Ratios for β_i for all species are 1.51 times greater than ratios for F_i because Earth's mean molecular weight is less than Mars' by 1.51. Ratios of Earth relative to Mars for ρ_i (gaseous mass density) are the same as for n_i (number density) because ρ is proportional to n. There is much more N_2, O_2, and H_2O on Earth than on Mars (by factors of 10^3 to 10^4). There is more interest in the ratios of ρ_i and n_i, for oxygen and water vapor, because both gases have strong absorption at microwave frequencies. On Mars, the amounts of O_2 and H_2O are very small, and the question is how much smaller the atmospheric attenuation is in comparison with Earth.

Table 2. Surface atmospheric parameters at Mars and Earth.

Planet	P, pressure, mb	T, temperature, K	M, mean molecule weight, g/mole	ρ, mass density, kg/m^3	N, number density, m^{-3}	V_m, mole volume, m^3/kmole	H, scale height, km
Mars	6.1	210	43.34	0.021	2.85×10^{23}	2.1×10^3	∼11.1
Earth	1013	300	28.61	1.29	2.7×10^{25}	22	∼9.5

Table 3. Ratios of atmospheric compositions between Earth and Mars.

Ratio (Earth–Mars)	CO_2	N_2	Ar	O_2	CO	H_2O
For F_i (fraction by volume)	4.2×10^{-4}	28.9	0.58	161	2.4×10^{-4}	33.3
For β_i (fraction by weight)	6.4×10^{-4}	44	0.88	244	3.9×10^{-4}	50.4
For ρ_i and n_i (density)	0.04	2704	54	14,000	0.024	3068

The total atmospheric attenuation, using equations and procedures developed by Waters [14], Liebe [15], and Ulaby et al. [16] have been calculated, using planetary atmospheric parameters listed in Tables 2 and 3. The total Martian atmospheric absorption coefficient is a combination of both H_2O and O_2 [16]:

$$\kappa_a(f) = \kappa_{H_2O}(f) + \kappa_{O_2}(f) \quad \text{dB/km} \tag{5}$$

Figure 2 shows the calculated specific atmospheric attenuation for a horizontal path at the Earth's surface and at Mars' surface. The plots only give a microwave frequency range less than 350 GHz. Above 350 GHz (in the far infrared), absorption spectral lines from all species are so complicated that we do not describe them. The dotted lines are for O_2 absorption only. There are two oxygen absorption peaks at 60 and 118.8 GHz, respectively. The dashed lines are for water vapor only. The water-vapor absorption peaks are at 22.2, 183.3, and 323.8 GHz. The solid lines are for both combined.

It is found that the attenuation values due to oxygen at Mars are reduced by a factor of 14,000 relative to Earth. This factor is the ratio ρ_{O_2} (oxygen density ratio) between Earth's atmosphere and Mars' atmosphere at the surface. The water-vapor attenuation at Mars is lower by a factor of 3068 than at Earth. In this article, the radio emission from clouds and fogs is neglected because both are so thin on Mars.

2. Optical Depth (Or Opacity) Along the Zenith [14,15]. The optical depth due to atmospheric gaseous absorption is

$$e^{-\tau} = e^{-A(f)/4.34} = 10^{-A(f)/10} \tag{6}$$

$$\tau(f) = \frac{A(f)}{4.34} \tag{7}$$

where τ is in units of nepers and $A(f)$ is in dB.

Assuming a form of $\kappa_g(z) = \kappa_a e^{-z/H_g}$, a one-way vertical gaseous attenuation is

$$A_0(f) = \int_0^\infty \kappa_g(f,z)dz = \kappa_a(f)H_g \tag{8}$$

where κ_g is the specific attenuation (dB/km) profile, H_g is the scale height of absorption gases, and κ_a is the surface specific attenuation (dB/km), shown in Fig. 2.

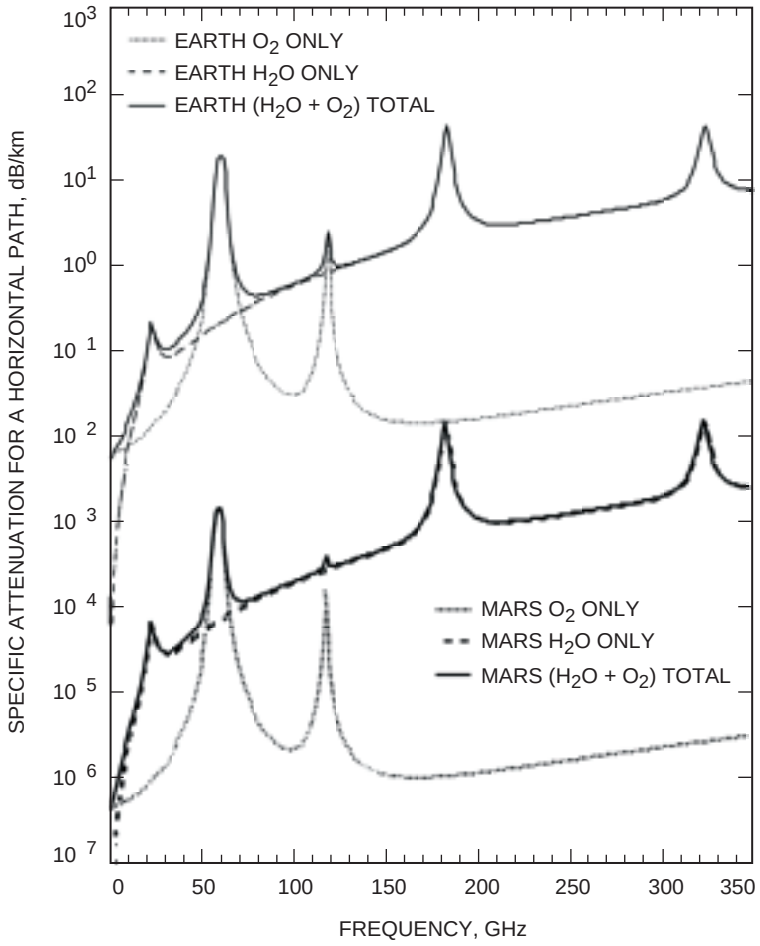

Fig. 2. Gaseous specific absorption attenuation, $_a(f)$, by water vapor, oxygen, and both at the surfaces of Earth and Mars. The upper three plots are for attenuation at Earth, while the lower three thicker plots are for Mars.

At Ka-band (32 GHz), the total zenith attenuation of the Martian atmosphere is estimated to be about 0.0003 dB. By comparison, in the Earth's atmosphere, the attenuation is about 0.3 dB. At higher frequencies (e.g., 100 GHz), the Martian atmospheric attenuation increases to 0.003 dB. Such a small attenuation is negligible for telecommunications.

For an oblique path with zenith angle θ, when $\theta < 70$ deg, the opacity may be simply expressed as

$$\tau(\theta) = \tau_0 \sec\theta \tag{9}$$

where τ_0 is defined as an integration of the absorption coefficient over a vertical path from the surface to infinity. Thus, an oblique path will have greater attenuation.

B. Mars Surface Emission

It is expected that Mars has a larger surface emissivity (and hence higher brightness temperatures) than Earth because land surfaces have lower dielectric constants than water surfaces. So far, no water surface has been detected on Mars. The soil's moisture and surface roughness also affect the emissivity.

The brightness temperature decreases as moisture content increases. If surface roughness is higher, the brightness temperature also increases.

Surfaces of Mars are filled with vast sand dune fields, various wind-eroded hills, and drifts of fine-grained material due to wind processes. The only three sites on Mars viewed close up show surfaces sprinkled with rocks in the centimeter-to-meter size range. In some areas, bedrock can occasionally be seen [17,18]. At the Mars Pathfinder site, the images revealed a rocky plain (about 20 percent covered by rocks) that appears to have been deposited and shaped by catastrophic floods. Large rocks are flat-topped and often perched on the surface. Between the rocks are mostly fine-grained ($<$100 μm) materials. Soils vary from bright-red dust to darker-gray material. Their composition is mainly sulfur, iron, magnesium, and silicon [19].

In general, lower material densities have lower reflectivity, ρ, for a given composition. For example, a solid rock has $\rho \sim 0.15$ to 0.25, while typical soils are in the range of $\rho \sim 0.03$ to 0.07. The Martian surface has a diverse structure; depending on location, the reflectivity covers at least 0.03 to 0.25 [18,20]. Thus, surface emissivity is $\varepsilon = 1 - \rho$, with a range from 0.75 to 0.97. Both parameters are functions of radio frequency. The brightness temperature of the Martian surface is εT_s, where T_s is the surface temperature of Mars. Ocean water has higher reflectivity and lower emissivity.

Temperatures at the Martian surface depend on latitude, season, and local time. Both hemispheres also have different temperatures. The lowest temperatures occur at the south pole during winter, where they fall as low as 148 K, the frost-point of CO_2. The highest temperatures are at southern low latitudes in summer, which may reach as high as 295 K. Representative diurnal variations of Mars' temperatures based on Viking measurements are shown in Fig. 3. The model also shows the local time changes in the temperature profiles in the lowest 8 km. The temperature reached its maximum of 238 K every day at 2 p.m. local solar time and its minimum of 190 K just before sunrise. In the lowest 4 km, there is a boundary layer that is strongly influenced by radiative exchange with the ground and in which a strong nighttime inversion forms. All emission parameter ranges are listed in Table 4, where Mars' values for ε and ρ were obtained from Earth-based radar observations in frequency ranges from UHF- to Ka-bands. The dust emission on the Martian surface is ignored in this article.

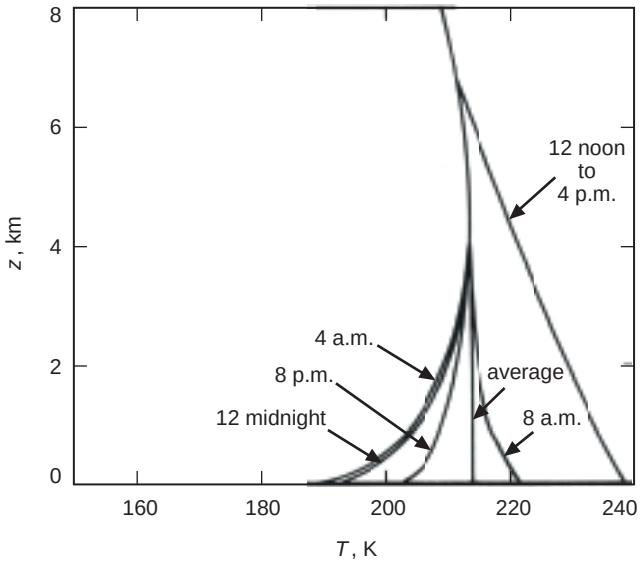

Fig. 3. Models of Martian atmosphere surface temperature, *T*, variation and temperature profiles in the lowest 8 km as a function of altitude, *z* [21].

Table 4. Parameter values and ranges on Mars and Earth.

Parameter	Mars	Earth
ε	0.75–0.97	0.40–0.97
ρ	0.03–0.25	0.03–0.60
T_s	215 (184–242) K	300 (250–320) K
T_a	200 K	230 K
H_g	11.1 km	9.5 km

C. Extra-Martian Emissions (Sky Temperature)

These emissions are basically the same as those extra-terrestrial emissions seen from Earth [22]. Emissions include cosmic and galactic noise. The cosmic radiation contribution has an effective brightness temperature of 2.0 to 2.7 K [23]. The galactic contribution is due to radiation from our own galaxy. It has a maximum in the direction of the center of the galaxy and a minimum in the direction of the galactic pole [24]. The frequency dependence of galactic brightness temperature varies between $f^{2.5}$ and f^3. Above 5 GHz, it may be neglected on Earth in comparison with atmospheric emission. The brightness temperature of the "quiet" Sun decreases rapidly with increasing frequency from about 10^6 K at 100 MHz down to about 10^4 K at 10 GHz. The Sun effect has been neglected in this article. These variations with frequency are shown in Fig. 4.

IV. Resultant Antenna Temperatures

Using the surface temperature, atmospheric temperature, and sky temperature given in the last section, the Martian brightness temperature and antenna temperature in ground and space have been calculated. All radiation parameters and calculated brightness temperatures for both Mars and Earth are shown in Table 5. In the table, all parameters are given by their average values, even though they have a broad range. For example, at Earth's ocean surface, which covers 70 percent of Earth's surface, there is a higher reflectivity coefficient, ρ, and lower emissivity, ε. Thus, on a global average, Earth has lower surface emissivity than does the Martian surface. However, certain areas on Earth, such as forest and high vegetation areas, have very high emissivity (almost 1). At Mars' surface, rocks usually have lower emissivity than desert sands on average over all the surface. Both surface reflectivity and emissivity have a radio frequency dependence; the emissivity coefficient increases as radio frequency increases (the ratio of surface roughness to wavelength increases). The gaseous attenuation, $A_0(f)$, and optical depth, $\tau_0(f)$, shown in Table 5 are for a vertical path. It can be seen that there is a significant difference in both parameters between Earth and Mars. The optical depth at Mars is less than that at Earth by about four orders of magnitude. Because of strong absorption, Earth's atmosphere is an important source of background noise temperature. In contrast, the very thin Martian atmosphere is transparent and almost can be neglected. Sky brightness temperatures for both planets are essentially the same as shown in Fig. 4. Upwelling and downwelling brightness temperatures are averaged over all longitudes (on Earth) and local times (on Mars). Upwelling temperatures at low latitudes have large fluctuations (about ± 15 percent), while downwelling temperatures have less fluctuation (± 5 percent). Mars' downwelling brightness temperature is the same as its sky temperature, $T_{\text{sky}}e^{-\tau}$, because of its almost transparent atmosphere. On Earth, this temperature is significantly larger than the sky temperature because of the large atmospheric emission contribution, especially at Ka-band.

When using Eq. (3) to calculate the upwelling brightness temperature, it is found that on Earth a longitudinal variation is more important than a local time variation for a geosynchronous orbit, where the satellite is above the Earth's equator. Diurnal temperature variation at the Earth's surface may have a ± 15 percent variation, while the emissivity coefficient may change by a factor of two from ocean surface

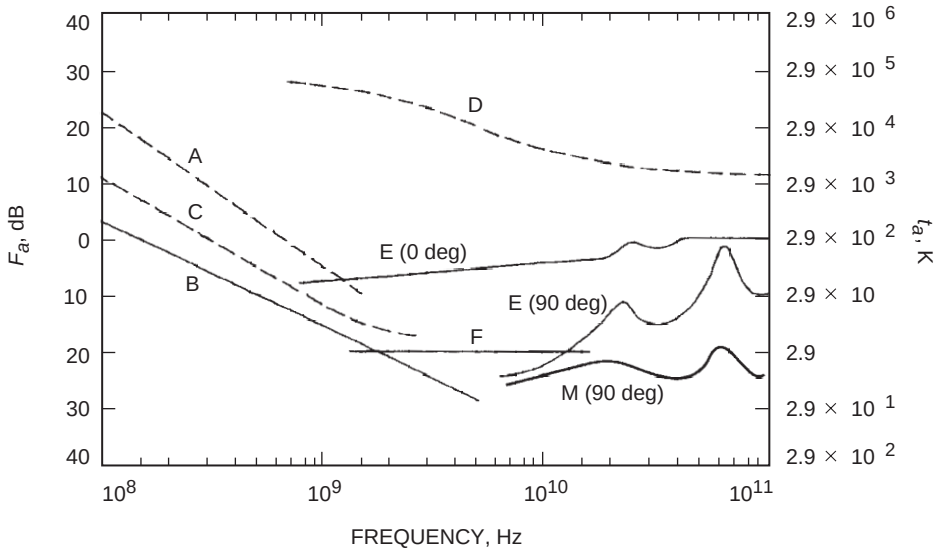

Fig. 4. External noise figure F_a, dB, and sky temperature t_a, K, versus frequency (0.1–100 GHz), where A = estimated man-made noise on Earth, B = galactic noise, C = galactic noise (toward the galactic center with infinitely narrow beamwidth), D = quiet Sun (0.5-deg beamwidth directed at the Sun), E = Earth atmosphere radiation (0-deg and 90-deg elevation angles), F = black body (2.7-K) radiation, and M = Martian atmospheric radiation.

Table 5. Average radiation parameters and brightness temperature for various frequency bands for Mars and Earth.

Parameter/ temperature	Planet	UHF-band	S-band	X-band	Ka-band
Average emissivity, ε	Mars	0.9	0.91	0.92	0.93
	Earth	0.6	0.62	0.64	0.68
Average reflectivity, ρ	Mars	0.1	0.09	0.08	0.07
	Earth	0.4	0.38	0.36	0.32
Vertical attenuation,	Mars	0.4×10^{-4}	0.8×10^{-4}	1.2×10^{-4}	3.0×10^{-4}
$A_0(f)$, dB	Earth	0.04	0.08	0.12	0.32
Zenith optical depth,	Mars	0.1×10^{-4}	0.2×10^{-4}	0.3×10^{-4}	0.7×10^{-4}
τ_0, neper	Earth	0.01	0.02	0.03	0.07
Sky brightness	Mars	29	4.7	5.0	3.0
temperature, T_{sky}	Earth	29	4.7	5.0	13
Upwelling brightness	Mars	189	191	193	195
temperature, T_{B_u}	Earth	182	188	196	210
Downwelling brightness	Mars	29	2.9	2.9	2.9
temperature, T_{B_d}	Earth	40	22	32	117

to land surface longitudinally, due to different land fractions on Earth. At Mars, the local time variation of surface temperature becomes an important factor. Because no water surfaces exist on Mars, there is a relatively large and constant emissivity coefficient on a global average (average $\varepsilon \geq 0.9$). The very thin atmosphere makes its optical depth almost zero ($\tau \approx 0$). The upwelling brightness temperature at Mars is directly controlled by the surface temperature as $T_{B_u} \approx \varepsilon T_s$. Thus, we expect that T_{B_u} on Earth has a strong longitudinal dependence, as shown in the study of Njoku et al. [3] for a geosynchronous orbit satellite, while T_{B_u} at Mars has large local time and latitudinal variations. However, for a general antenna viewing Earth with a narrow beam, which could be in a variety of orbits, the antenna temperature variation is not a function of longitude, but depends on the specific surface types.

Local time and latitudinal variations of Martian atmospheric temperature at one scale height are not clear, where the temperature is assumed to be a constant 200 K (see Fig. 3). Downwelling brightness temperature at Mars (for an upward-looking antenna) is primarily controlled by the sky temperature (see Fig. 4); therefore, there is no local time variation for it.

Figure 5 shows the local time variations of upwelling brightness temperature for a downward-looking antenna for four frequency bands at a low Martian latitude (30 deg N). The temperatures have large local time variations. The deviations can be as large as ±15 percent relative to their averages. Temperatures have small increases with increasing frequency. Similar to surface temperature profiles, at 0700 hours local time the brightness temperature reaches its minimum, while at 1300 hours local time there is a maximum. Figure 6 shows latitudinal variations of upwelling brightness temperature for 8.4 GHz (X-band) during summer in the southern hemisphere. At 60-deg north latitude, the temperature will fall below the CO_2 ice point. At the same time, at 30-deg south latitude, the temperature will reach its maximum. This is a 120-K temperature difference in the upwelling brightness temperature.

Average noise temperatures received by both downward-looking and upward-looking antennas are listed in Table 6. For a downward-looking antenna, antenna temperatures increase with increasing frequency on both planets, since emissivity coefficients and upwelling brightness temperature increase with frequency. The total noise temperature on Mars is about the same as the Earth's for all frequency bands but

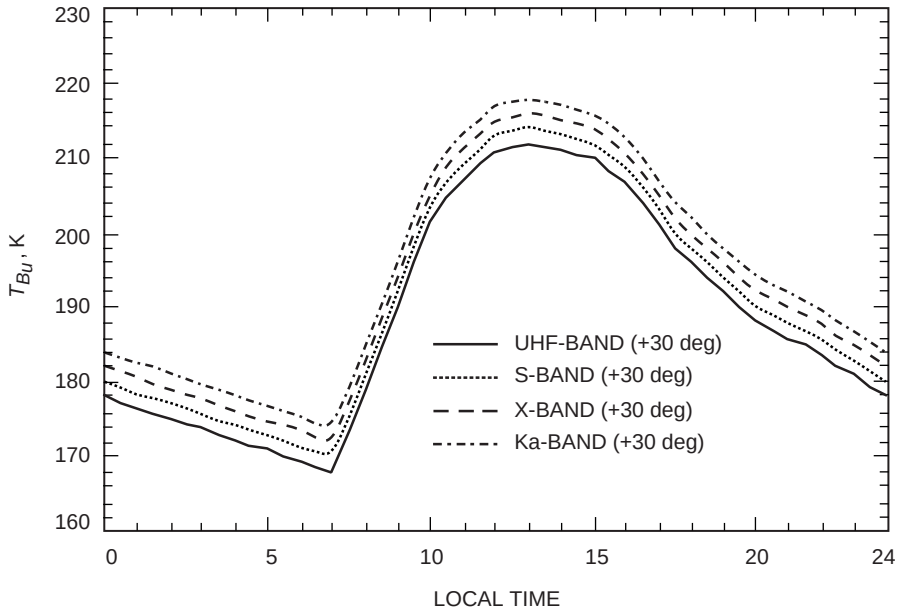

Fig. 5. Upwelling brightness temperature variations with local time at Mars 30-deg-N latitude for different frequency bands during the summer in the southern hemisphere.

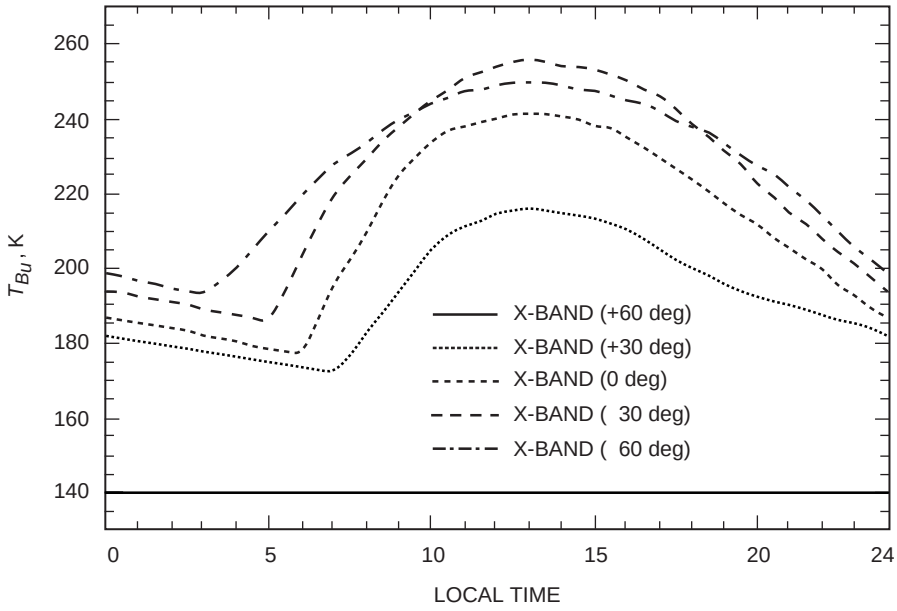

Fig. 6. Upwelling brightness temperature variations with Mars latitudes for X-band when the southern hemisphere is in summer.

Table 6. Average antenna temperature for various frequency bands for Mars and Earth.

Antenna/ receiver	Planet	UHF-band temperature, K	S-band temperature, K	X-band temperature, K	Ka-band temperature, K	Omni-directional temperature, K
Downward-looking	Mars	155	185	191	193	—
	Earth	150	180	193	210	—
Upward-looking	Mars	54	9	4	3	79
	Earth	88	27	32	117	85
Receiver thermal temperature	Mars	450	450	450	450	450

with ±15 percent deviations. For an upward-looking antenna based on the Martian surface, antenna temperature variation with frequency is dependent on both sky temperature and atmospheric emission. The noise temperature on Mars is below that at Earth with ±5 percent deviation. This is obtained through an integration in all directions over the background brightness temperature, but the main contribution comes from the direction of the antenna's main beam. For a downward-looking antenna in Mars orbit, at lower frequency bands (e.g., UHF-band), the antenna temperature in Table 6 is lower than the upwelling brightness temperature in Table 5. Because of the larger beamwidth, the integration is performed over a larger surface area seen by the main lobe at UHF-band. The emissions from areas away from the nadir of the spacecraft will propagate obliquely into the receiving antenna with a larger zenith angle, as given in Eq. (9). Thus, the main term for upwelling temperature, $\varepsilon T_{B_u} e^{-\tau}$, becomes smaller with a larger $\tau(\theta)$. However, for an upward-looking antenna based on the Martian surface, higher upwelling brightness temperatures still have significant effects through the antenna's side lobes. As a result, the integrated antenna temperatures at both UHF- and S-bands are higher than their downwelling brightness temperatures. For higher frequencies (e.g., Ka-band), there is a very narrow pencil beam for its main lobe, which vertically illuminates a small area. Under this condition, the antenna temperature is almost

the same as the surface brightness temperature, as shown in Table 6. Receiver system thermal noise temperatures[3] for Mars missions are also listed in the bottom line of the table; they are far higher than the antenna background noise temperature that was obtained from this study.

V. Summary

Mars and Earth environments are significantly different in their surface features and atmospheres. Radio noise emissions at Mars basically include three types of sources: Martian atmospheric emission, noise from the Martian surface, and extra-Martian sources. In this article, radio noise temperatures and optical depths of the Martian atmosphere have been estimated. Compared with Earth, the Martian atmosphere has a very low density (especially in O_2 and water vapor contents). Its gaseous absorption and radiation are very low in the microwave frequency range. Its contribution to the noise temperature is almost negligible. Mars' atmospheric optical depth is less than Earth's by about four orders in magnitude. This makes it almost transparent to Mars' surface and sky emissions. Mars has lower surface temperatures than Earth, but higher average surface emissivity due to the roughness of soil and rocks on the surface. The sky temperature is basically the same as those extra-terrestrial emissions seen from Earth.

A Martian atmospheric gaseous attenuation model has been developed. One-way vertical optical depths at various frequency bands have been obtained. It has been found that the main contributor to upwelling brightness temperature at Mars is surface temperature, with strong local time and latitudinal variations. The downwelling brightness temperature is dominated by sky temperature. The actual radio noise contributing to the antenna temperature is also a function of antenna orientation, elevation angle, and gain pattern. Antenna temperatures for two simple pointing cases have been calculated through an integration over all directions. For a downward-looking antenna in Mars orbit, the total noise temperature is about the same as Earth's for all frequency bands, with ±15 percent deviations. For an upward-looking antenna based on the Martian surface, the noise temperature is below that at Earth. The differences increase with increasing frequency, from UHF-band (a 2-dB ratio) to Ka-band (a 16-dB ratio). Both antenna temperatures are below the receiver system noise temperature.

Acknowledgments

We would like to thank Dr. Nasser Golshan for his help in this study. We are also grateful to Dr. Anil Kantak for reviewing this article.

References

[1] C. Ho, N. Golshan, and A. Kliore, *Radio Wave Propagation Handbook for Communication on and around Mars, Part I: Propagation through the Mars Environment*, NASA Technical Publication TP2000-209756, Jet Propulsion Laboratory, Pasadena, California, 2001 (in press).

[3] K. Nelson, W. Horne, and V. Ayala, "Review of Frequency Choice for Mars In Situ Link," Stanford Telecom Memorandum (internal document), Reston, Virginia, December 2, 1999.

[2] G. Schiavon, P. Ferrazzoli, D.Solimini, P. Maagt, and J. P. V. Baptista, "A Global High-Resolution Microwave Emission Model for the Earth," *Radio Science*, vol. 33, pp. 753–766, 1998.

[3] E. G. Njoku and E. K. Smith, "Microwave Antenna Temperature of the Earth from Geostationary Orbit," *Radio Science*, vol. 20, pp. 591–599, 1985.

[4] "Radio Emission from Natural Source in the Frequency Range above 50 MHz," Report 720-2, CCIR, 1986.

[5] "Mathematical Model of Average and Related Radiation Patterns for Line-of-Sight Point-to-Point Radio-Relay System Antennas for Use in Certain Coordination Studies and Interference Assessment in the Frequency Range from 1 GHz to About 70 GHz," Recommendation ITU-R F.1245-1, ITU-R, 2000.

[6] "Attenuation by Atmospheric Gases," Report 719-2, CCIR, pp. 167, in *Propagation in Non-ionized Media, Recommendation and Report of the CCIR*, vol. V, Geneva: ITU, 1986.

[7] T. Owen, "The Composition and Early History of the Atmosphere of Mars," in *Mars*, H. H. Kieffer, B. M. Jakosky, C. W. Snyder, and M. S. Mathews, eds., Tucson, Arizona: University of Arizona Press, p. 818, 1992.

[8] A. O. Nier and M. B. McElroy, "Composition and Structure of Mars' Upper Atmosphere: Results from the Neutral Mass Spectrometers on Viking 1 and 2," *J. Geophys. Res.*, vol. 82, p. 4341, 1977.

[9] M. B. McElroy, T. Y. Kong, and Y. L. Yung, "Photochemistry and Evolution of Mars' Atmosphere: A Viking Perspective," *J. Geophys. Res.*, vol. 82, p. 4379, 1977.

[10] P. E. Doms, "Water Vapor in the Martian Atmosphere: A Discussion of the Viking Data," in *The Mars Reference Atmosphere*, Special Issue in COSPAR, A. J. Kliore, ed., *Adv. Space Res.*, vol. 2, 1982.

[11] M. B. McElroy and J. C. McConnell, "Dissociation of CO_2 in the Martian Atmosphere," *J. Atmos. Sci.*, vol. 28, p. 879, 1971.

[12] Y. L. Yung, D. F. Strobel, T. Y. Kong, and M. B. McElroy, "Photochemistry of Nitrogen in the Martian Atmosphere," *Icarus*, vol. 30, p. 2641, 1977.

[13] C. B. Famer and P. E. Doms, "Global Seasonal Variation of Water Vapor on Mars and the Implications for Permafrost," *J. Geophys. Res.*, vol. 84, p. 2881, 1979.

[14] J. W. Waters, "Absorption and Emission by Atmospheric Gases," in *Astrophysics—Part B: Radio Telescopes*, vol. 12, in *Methods of Experimental Physics*, M. L. Meeks, ed., New York: Academic Press, p. 142, 1976.

[15] H. J. Liebe, "Modelling Attenuation and Phase of Radio Waves in Air at Frequencies below 1000 GHz," *Radio Science*, vol. 16, p. 1183, 1981.

[16] F. T. Ulaby, R. K. Moore, and A. K. Fung, "Microwave Interaction with Atmospheric Constituents," in *Microwave Remote Sensing: Active and Passive, Vol 1: Microwave Remote Sensing Fundamentals and Radiometry*, F. T. Ulaby, R. K. Moore, and A. K. Fung, eds., Reading, Massachusetts: Addison-Wesley Publishing Company, Inc., p. 256, 1981.

[17] M. H. Carr, *The Surface of Mars*, Westford, Massachusetts: Yale University Press, 1981.

[18] R. A. Simpson, J. K. Harmon, S. H. Zisk, T. W. Thompson, and D. O. Muhleman, "Radar Determination of Mars Surface Properties," in *Mars*, H. H. Kieffer, B. M. Jakosky, C. W. Snyder, and M. S. Mathews,, eds., Tucson, Arizona: University of Arizona Press, p. 652, 1992.

[19] M. C. Malin, M. H. Carr, G. E. Danielson, M. E. Davies, W. K. Hartmann, A. P. Ingersoll, P. B. James, H. Masursky, A. S. McEwen, L. A. Soderblom, P. Thomas, J. Veverka, M. A. Caplinger, M. A. Ravine, T. A. Soulanille, and J. L. Warren, "Early Views of the Martian Surface from the Mars Orbiter Camera of Mars Global Surveyor," *Science*, vol. 279, p. 1681, 1998.

[20] P. R. Christensen and H. J. Moore, "The Martian Surface Layer," in *Mars*, H. H. Kieffer, B. M. Jakosky, C. W. Snyder, and M. S. Mathews, eds., Tucson, Arizona: University of Arizona Press, p. 686, 1992.

[21] A. Seiff, "Post-Viking Models for the Structure of the Summer Atmosphere of Mars," in *The Mars Reference Atmosphere*, Special Issue in COSPAR, A. J. Kliore, ed., *Adv. Space Res.*, vol. 2, 1982.

[22] "Use of Radio-Noise Data in Spectrum Utilization Studies," Recommendation 508, CCIR, 1978.

[23] C. T. Stelzried, *The Deep Space Network—Noise Temperature Concepts, Measurements, and Performance*, JPL Publication 82-33, Jet Propulsion Laboratory, Pasadena, California, September 15, 1982.

[24] J. D. Kraus, *Radio Astronomy*, 2nd ed., Powell, Ohio: Cygnus-Quasar Books, 1986.